The Gut Bacterial Community Potentiates *Clostridioides difficile* Infection Severity

Nicholas A. Lesniak,[a] Alyxandria M. Schubert,[a] Kaitlin J. Flynn,[a] Jhansi L. Leslie,[a*] Hamide Sinani,[a] Ingrid L. Bergin,[c] Vincent B. Young,[a,b] Patrick D. Schloss[a]

[a]Department of Microbiology and Immunology, University of Michigan, Ann Arbor, Michigan, USA
[b]Division of Infectious Diseases, Department of Internal Medicine, University of Michigan Medical School, Ann Arbor, Michigan, USA
[c]Unit for Laboratory Animal Medicine, University of Michigan, Ann Arbor, Michigan, USA

ABSTRACT The severity of *Clostridioides difficile* infections (CDI) has increased over the last few decades. Patient age, white blood cell count, and creatinine levels as well as *C. difficile* ribotype and toxin genes have been associated with disease severity. However, it is unclear whether specific members of the gut microbiota are associated with variations in disease severity. The gut microbiota is known to interact with *C. difficile* during infection. Perturbations to the gut microbiota are necessary for *C. difficile* to colonize the gut. The gut microbiota can inhibit *C. difficile* colonization through bile acid metabolism, nutrient consumption, and bacteriocin production. Here, we sought to demonstrate that members of the gut bacterial communities can also contribute to disease severity. We derived diverse gut communities by colonizing germfree mice with different human fecal communities. The mice were then infected with a single *C. difficile* ribotype 027 clinical isolate, which resulted in moribundity and histopathologic differences. The variation in severity was associated with the human fecal community that the mice received. Generally, bacterial populations with pathogenic potential, such as *Enterococcus*, *Helicobacter*, and *Klebsiella*, were associated with more-severe outcomes. Bacterial groups associated with fiber degradation and bile acid metabolism, such as *Anaerotignum*, *Blautia*, *Lactonifactor*, and *Monoglobus*, were associated with less-severe outcomes. These data indicate that, in addition to the host and *C. difficile* subtype, populations of gut bacteria can influence CDI disease severity.

IMPORTANCE *Clostridioides difficile* colonization can be asymptomatic or develop into an infection ranging in severity from mild diarrhea to toxic megacolon, sepsis, and death. Models that predict severity and guide treatment decisions are based on clinical factors and *C. difficile* characteristics. Although the gut microbiome plays a role in protecting against CDI, its effect on CDI disease severity is unclear and has not been incorporated into disease severity models. We demonstrated that variation in the microbiome of mice colonized with human feces yielded a range of disease outcomes. These results revealed groups of bacteria associated with both severe and mild *C. difficile* infection outcomes. Gut bacterial community data from patients with CDI could improve our ability to identify patients at risk of developing more severe disease and improve interventions that target *C. difficile* and the gut bacteria to reduce host damage.

KEYWORDS CDI, *Clostridium difficile*, human microbiome, humanized mice, microbial ecology

C*lostridioides difficile* infections (CDI) have increased in incidence and severity since *C. difficile* was first identified as the cause of antibiotic-associated pseudomembranous colitis (1). CDI disease severity can range from mild diarrhea to toxic megacolon and death. The Infectious Diseases Society of America (IDSA) and Society for

Healthcare Epidemiology of America (SHEA) guidelines define severe CDI in terms of a white blood cell count greater than 15,000 cells/mm^3 and/or a serum creatinine level of greater than 1.5 mg/dL. Patients who develop shock or hypotension, ileus, or toxic megacolon are considered to have fulminant CDI (2). Since these measures are CDI outcomes, they have a limited ability to predict risk of severe CDI when the infection is first detected. Schemes have been developed to score a patient's risk for severe CDI outcomes based on clinical factors but have not been robust for broad application (3). Thus, we have limited ability to prevent patients from developing severe CDI.

Missing from CDI severity prediction models are the effects of the indigenous gut bacteria. *C. difficile* interacts with the gut community in many ways. The indigenous bacteria of a healthy intestinal community prevent *C. difficile* from infecting the gut (4). A range of mechanisms can disrupt this inhibition, including antibiotics, medications, and dietary changes, and lead to increased susceptibility to CDI (5–7). Once *C. difficile* overcomes the inhibition and colonizes the intestine, the indigenous bacteria can either promote or inhibit *C. difficile* by producing molecules or modifying the environment (8, 9). Bile acids metabolized by the gut bacteria can inhibit *C. difficile* growth and affect toxin production (4, 10, 11). Bacteria in the gut also can compete more directly with *C. difficile* through antibiotic production or nutrient consumption (12–14). While the relationship between the gut bacteria and *C. difficile* has been established, the effect the gut bacteria can have on CDI disease severity is unclear.

Recent studies have demonstrated that when mice with diverse microbial communities were challenged with a high-toxigenicity strain, it resulted in varied disease severity (15), and when challenged with a low-toxigenicity strain, members of the gut microbial community were associated with variation in colonization (16). Here, we sought to further elucidate the relationship between members of the gut bacterial community and CDI disease severity when challenged with a highly toxigenic strain, *C. difficile* ribotype 027 (RT027). We hypothesized that since specific groups of gut bacteria affect the metabolism of *C. difficile* and its clearance rate, specific groups of bacteria are associated with variation in CDI disease severity. To test this hypothesis, we colonized germfree C57BL/6 mice with human fecal samples to create varied gut communities. We then challenged the mice with *C. difficile* RT027 and followed the mice for the development of severe outcomes of moribundity and histopathologic cecal tissue damage. Since the murine host and *C. difficile* isolate were the same and only the gut community varied, the variation in disease severity we observed was attributable to the gut microbiome.

RESULTS

***C. difficile* is able to infect germfree mice colonized with human fecal microbial communities without antibiotics.** To produce gut microbiomes with greater variation than those found in conventional mouse colonies, we colonized germfree mice with bacteria from human feces (17). We inoculated germfree C57BL/6 mice with homogenized feces from each of 15 human fecal samples via oral gavage. These human fecal samples were selected because they represented diverse community structures based on community clustering (18). After the gut communities had colonized for 2 weeks, we confirmed them to be *C. difficile* negative by culture (19). We then surveyed the bacterial members of the gut communities by 16S rRNA gene sequencing of murine fecal pellets (Fig. 1A). The bacterial communities from each mouse grouped more closely to those communities from mice that received the same human fecal donor community than to the mice who received a different human fecal donor community (Fig. 1B). The communities were primarily composed of populations of *Clostridia*, *Bacteroidia*, *Erysipelotrichia*, *Bacilli*, and *Gammaproteobacteria*. However, the gut bacterial communities of each donor group of mice harbored unique relative abundance distributions of the shared bacterial classes.

Next, we tested this set of mice with their human-derived gut microbial communities for susceptibility to *C. difficile* infection. A typical mouse model of CDI requires pretreatment of conventional mice with antibiotics, such as clindamycin, to become susceptible to *C. difficile* colonization (20, 21). However, we wanted to avoid modifying the gut
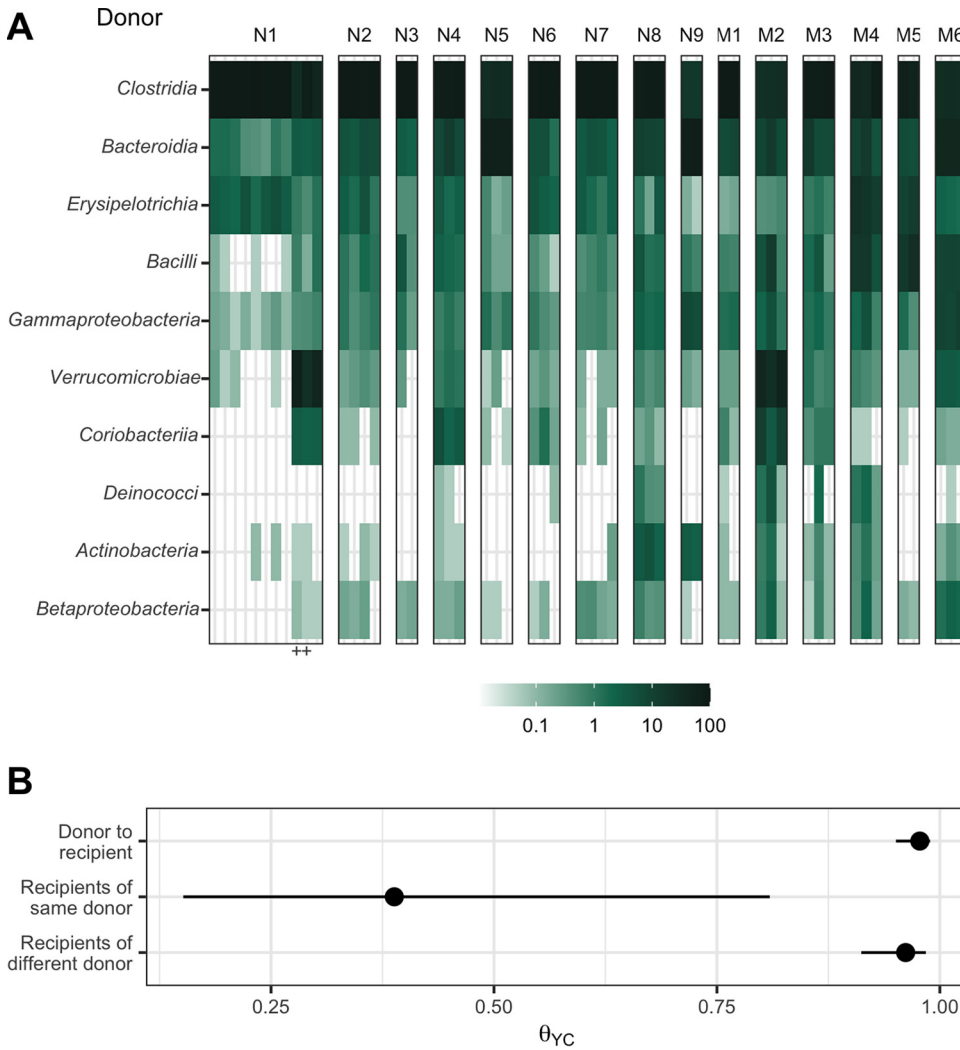
FIG 1 Human fecal microbial communities established diverse gut bacterial communities in germfree mice. (A) Relative abundances of the 10 most abundant bacterial classes observed in the feces of previously germfree C57BL/6 mice 14 days postcolonization with human fecal samples (i.e., day 0 relative to *C. difficile* challenge). Each column of abundances represents an individual mouse. Mice that received the same donor feces are grouped together and labeled above with a letter ("N" for nonmoribund mice and "M" for moribund mice) and number (ordered by mean histopathologic score of the donor group). "+" indicates the mice that did not have detectable *C. difficile* CFU (Fig. 2). (B) Medians (points) and interquartile ranges (lines) of β diversity (θ_{YC}) between an individual mouse and either all others that were inoculated with feces from the same donor or inoculated with feces from a different donor. The β diversity among the same-donor comparison group was significantly less than the β diversity of either the different-donor group or the overall donor community ($P < 0.05$, calculated by Wilcoxon rank sum test).

communities with an antibiotic to maintain their unique microbial compositions and eco-logical relationships. Since some of these communities came from people at increased risk of CDI, such as recent hospitalization or antibiotic use (18), we tested whether *C. difficile* was able to infect these mice without an antibiotic perturbation. We hypothesized that *C. difficile* would be able to colonize the mice who received their gut communities from a donor with a perturbed community. Mice were challenged with 10^3 *C. difficile* RT027 clinical isolate spores. The mice were followed for 10 days postchallenge, and their stool was collected and plated for *C. difficile* CFU to determine the extent of the infection. Surprisingly, communities from all donors were able to be colonized (Fig. 2). Two mice were able to resist *C. difficile* colonization: both received their community from donor N1 ("N" represents nonmoribund), which may be attributed to experimental variation since this group also had more mice. By colonizing germfree mice with different human fecal
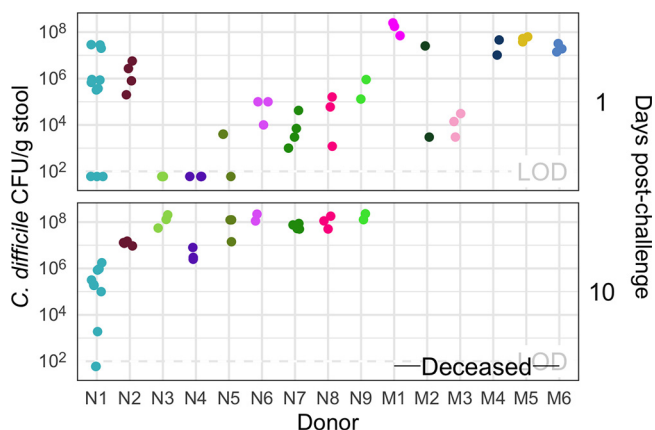
FIG 2 All donor groups resulted in *C. difficile* infection, but with different outcomes. The number of *C. difficile* CFU per gram of stool was measured the day after challenge with 10^3 *C. difficile* RT027 clinical isolate 431 spores and at the end of the experiment, 10 days postchallenge. Each point represents an individual mouse. Mice are grouped by donor and labeled by the donor letter ("N" for nonmoribund mice and "M" for moribund mice) and number (ordered by mean histopathologic score of the donor group). Points are colored by donor group. Mice from donor groups N1 through N6 succumbed to the infection prior to day 10 and were not plated on day 10 postchallenge. LOD, limit of detection. "—Deceased—" indicates mice were deceased at that time point, so no sample was available.

communities, we were able to generate diverse gut communities in mice, which were susceptible to *C. difficile* infection without further modification of the gut community.

Infection severity varies by initial community. After we challenged the mice with *C. difficile*, we investigated the outcome from the infection and its relationship to the initial community. We followed the mice for 10 days postchallenge for colonization density, toxin production, and mortality. Seven mice, with communities from donors N1, N3, N4, and N5 were not colonized at detectable levels on the day after *C. difficile* challenge but were infected ($>10^6$) by the end of the experiment. All mice that received their community from donors M1 through M6 ("M" represents moribund) succumbed to the infection and became moribund within 3 days postchallenge. The remaining mice, except the uninfected donor N1 mice, maintained *C. difficile* infection through the end of the experiment (Fig. 2). At 10 days postchallenge, or earlier for the moribund mice, mice were euthanized, fecal material was assayed for toxin activity, and cecal tissue was collected and scored for histopathologic signs of disease (Fig. 3). Overall, there was greater toxin activity detected in the stool of the moribund mice (see Fig. S1 in the supplemental material). However, when looking at each group of mice, we observed a range of toxin activities for both the moribund and nonmoribund mice (Fig. 3A). Nonmoribund mice with communities from donors N2 and N5 through N9 had comparable toxin activity to the moribund mice at 2 days postchallenge. Additionally, not all moribund mice had toxin activity detected in their stool. Next, we examined the cecal tissue for histopathologic damage. Moribund mice had high levels of epithelial damage, tissue edema, and inflammation (Fig. S2), similar to previously reported histopathologic findings for *C. difficile* RT027 (22). As observed with toxin activity, the moribund mice had higher histopathologic scores than the nonmoribund mice ($P < 0.001$). However, unlike the toxin activity, all moribund mice had consistently high histopathologic summary scores (Fig. 3B). The nonmoribund mice (representing donor groups N1 through N9) had a range of tissue damage from none detected to levels similar to those in the moribund mice, which grouped by community donor. Together, the toxin activity, histopathologic score, and moribundity showed variation across the donor groups but were largely consistent within each donor group.

Microbial community members explain variation in CDI severity. We next interrogated the bacterial communities at the time of *C. difficile* challenge (day 0) for their relationship to infection outcomes using linear discriminant analysis (LDA) effect size
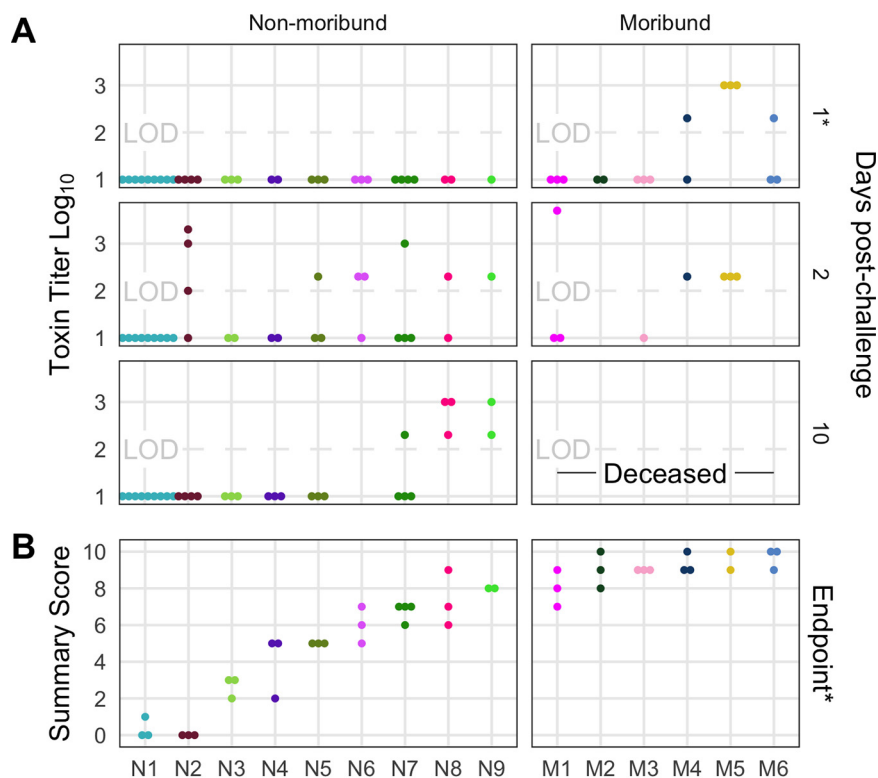
FIG 3 Histopathologic scores and toxin activities varied across donor groups. (A) Fecal toxin activity was detected in some mice post-*C. difficile* challenge in both moribund and nonmoribund mice. (B) Cecum scored for histopathologic damage from mice at the end of the experiment. Samples were collected for histopathologic scoring on day 10 postchallenge for nonmoribund mice or the day the mouse succumbed to the infection for the moribund group (day 2 or 3 postchallenge). Each point represents an individual mouse. Mice are grouped by donor and labeled by the donor letter ("N" for nonmoribund mice and "M" for moribund mice) and number (ordered by mean histopathologic score of the donor group). Points are colored by donor group. Mice in group N1 that have a summary score of 0 are the mice that did not have detectable *C. difficile* CFU (Fig. 2). Missing points are from mice that had insufficient fecal sample collected for assaying toxin or cecum for histopathologic scoring. *, significant difference between nonmoribund and moribund groups of mice by Wilcoxon test ($P < 0.002$).

(LEfSe) analysis to identify individual bacterial populations that could explain the variation in disease severity. We split the mice into groups by severity level based on moribundity or 10-day postinfection (dpi) histopathologic score for nonmoribund mice. This analysis revealed bacterial operational taxonomic units (OTUs) that were significantly different at the time of challenge by the disease severity (Fig. 4A). OTUs associated with *Akkermansia*, *Bacteroides*, *Clostridium sensu stricto*, and *Turicibacter* were detected at higher relative abundances in the mice that became moribund. OTUs associated with *Anaerotignum*, *Enterocloster*, and *Murimonas* were more abundant in the nonmoribund mice that would develop low intestinal injury. To understand the role of toxin activity in disease severity, we applied LEfSe to identify the OTUs at the time of challenge that most likely explain the differences between communities that had toxin activity detected at any time point and those that did not (Fig. 4B). An OTU associated with *Bacteroides*, OTU 7, which was associated with the presence of toxin, was also associated with moribundity. Likewise, OTUs associated with *Enterocloster* and *Murimonas* that were associated with no detected toxin also exhibited greater relative abundance in communities from nonmoribund mice with a low histopathologic score. We tested for correlations between the endpoint (10 dpi) relative abundances of OTUs and the histopathologic summary score (Fig. 4C). The endpoint relative abundance of *Bacteroides* OTU 17 was positively correlated with histopathologic score, as its day 0 relative abundance did with disease severity (Fig. 4A). The population of OTU 17 was
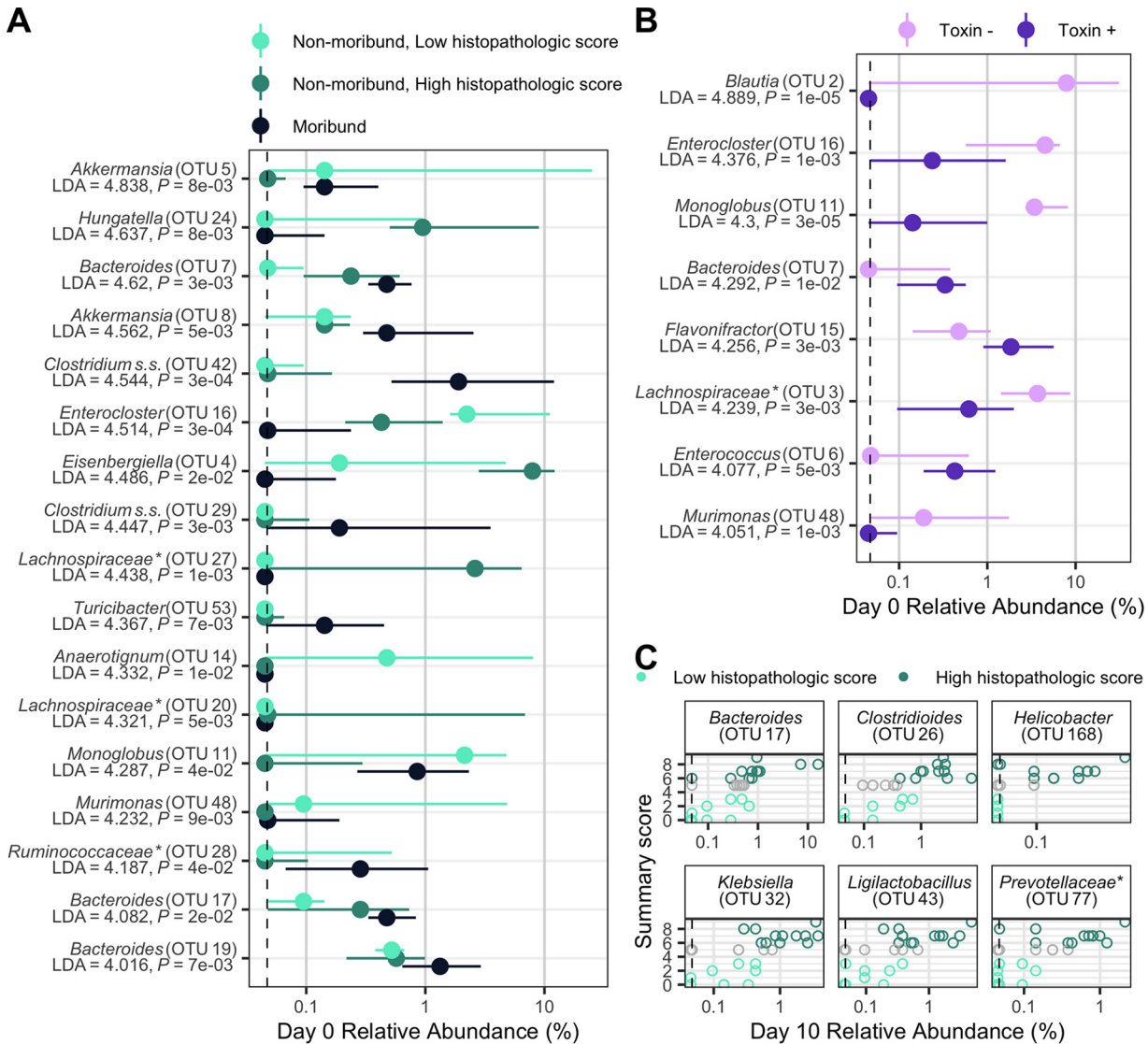
FIG 4 Individual fecal bacterial community members of the murine gut associated with *C. difficile* infection outcomes. (A and B) Relative abundance of OTUs at the time of *C. difficile* challenge (day 0) that varied significantly by the moribundity and histopathologic summary score or with detected toxin by LEfSe analysis. The median (points) and interquartile range (lines) are plotted. (A) Day 0 relative abundances were compared across infection outcome of moribund (colored black) or nonmoribund with either a high histopathologic score (score greater than the median score of 5, colored green) or a low histopathologic summary score (score less than the median score of 5, colored light green). (B) Day 0 relative abundances were compared between mice in which toxin activity was detected (Toxin +, colored dark purple) and which no toxin activity was detected (Toxin −, colored light purple). (C) Day 10 bacterial OTU relative abundances correlated with histopathologic summary score. Data for each mouse are plotted and colored according to their categorization in panel A. Points at the median score of 5 (gray points) were not included in panel A. Spearman's correlations were statistically significant after Benjamini-Hochberg correction for multiple comparisons. All bacterial groups are ordered by the LDA score. *, the bacterial group was unclassified at lower taxonomic classification ranks.

also increased in the group of mice with detectable toxin. We also tested for correlations between the endpoint relative abundances of OTUs and toxin activity, but none were significant. Finally, we tested for associations between temporal changes and disease severity (Fig. S4). Most groups of bacteria maintained higher relative abundance than the other outcome groups from day 0 through the end of the experiment. This analysis identified bacterial populations that were associated with the variation in moribundity, histopathologic score, and toxin.

We next determined whether, collectively, bacterial community membership and relative abundance could be predictive of the CDI disease outcome. We trained logistic regression models with bacterial community relative abundance data from the day of

colonization at each taxonomic rank to predict toxin, moribundity, and histopathologic summary score. We used the highest taxonomic classification rank that performed similar to lower ranks, which suggested the effect is associated with general attributes of the bacterial group, as opposed to specific functions of more refined grouping. For prediction of whether detectable toxin would be produced, microbial populations aggregated by genus rank classification performed similarly to models using lower taxonomic ranks (mean area under the receiver operating characteristic curve [AUROC] = 0.787 [Fig. S3]). *C. difficile* increased odds of producing detectable toxin when the community infected had less-abundant populations of *Monoglobus*, *Akkermansia*, *Extibacter*, *Intestinimonas*, and *Holdemania* and had more abundant populations of *Lachnospiraceae* (Fig. 5A). Next, we assessed the ability of the community to predict moribundity. Grouping of bacteria by order rank classification was sufficient to predict which mice would succumb to the infection before the end of the experiment (mean AUROC = 0.9205 [Fig. S3]). Many populations contributed to increased odds of moribundity (Fig. 5B). Populations related to *Bifidobacteriales* and *Clostridia* decreased the odds of a moribund outcome. Finally, the relative abundances of OTUs were able to predict a high or low histopathologic score 10 dpi (with histopathologic scores dichotomized as in previous analysis; mean AUROC = 0.99 [Fig. S3]). The model identified some similar OTUs to the LEfSe analysis, such as *Murimonas* (OTU 48), *Bacteroides* (OTU 7), and *Hungatella* (OTU 24). These models have shown that the relative abundances of bacterial populations and their relationships with each other could be used to predict the variation in moribundity, histopathologic score, and detectable toxin of CDI.

DISCUSSION

Challenging mice colonized with different human fecal communities with *C. difficile* RT027 demonstrated that variation in members of the gut microbiome affects *C. difficile* infection disease severity. Our analysis revealed an association between the relative abundance of bacterial community members and disease severity. Previous studies investigating the severity of CDI disease involving the microbiome have had a limited ability to interrogate this relationship between the microbiome and disease severity. Studies that have used clinical data have a limited ability to control variation in the host, microbiome, or *C. difficile* ribotype (23). Murine experiments typically use a single mouse colony and different *C. difficile* ribotypes to create differences in severity (24). Recently, our group has begun uncovering the effect microbiome variation has on *C. difficile* infection. We showed the variation in the bacterial communities between mice from different mouse colonies resulted in different clearance rates of *C. difficile* (16). We also showed varied abilities of mice to spontaneously eliminate *C. difficile* infection when they were treated with different antibiotics prior to *C. difficile* challenge (25). Overall, the results presented here have demonstrated that the gut bacterial community contributed to the severity of *C. difficile* infection.

C. difficile can lead to asymptomatic colonization or infections with severity ranging from mild diarrhea to death. Physicians use classification tools to identify patients most at risk of developing a severe infection using white blood cell counts, serum albumin level, or serum creatinine level (2, 26, 27). Those levels are driven by the activities in the intestine (28). Research into the drivers of this variation have revealed factors that make *C. difficile* more virulent. Strains are categorized for their virulence by the presence and production of the toxins TcdA, TcdB, and binary toxin and the strains' prevalence in outbreaks, such as ribotypes 027 and 078 (20, 29–32). However, other studies have shown that disease is not necessarily linked with toxin production (33) or the strain (34). Furthermore, there is variation in the genome, growth rate, sporulation, germination, and toxin production in different isolates of a strain (35–38). This variation may help explain why severe CDI prediction tools often miss identifying many patients with CDI that will develop severe disease (3, 24, 39, 40). Therefore, it is necessary to gain a full understanding of all factors contributing to disease variation to improve our ability to predict severity.
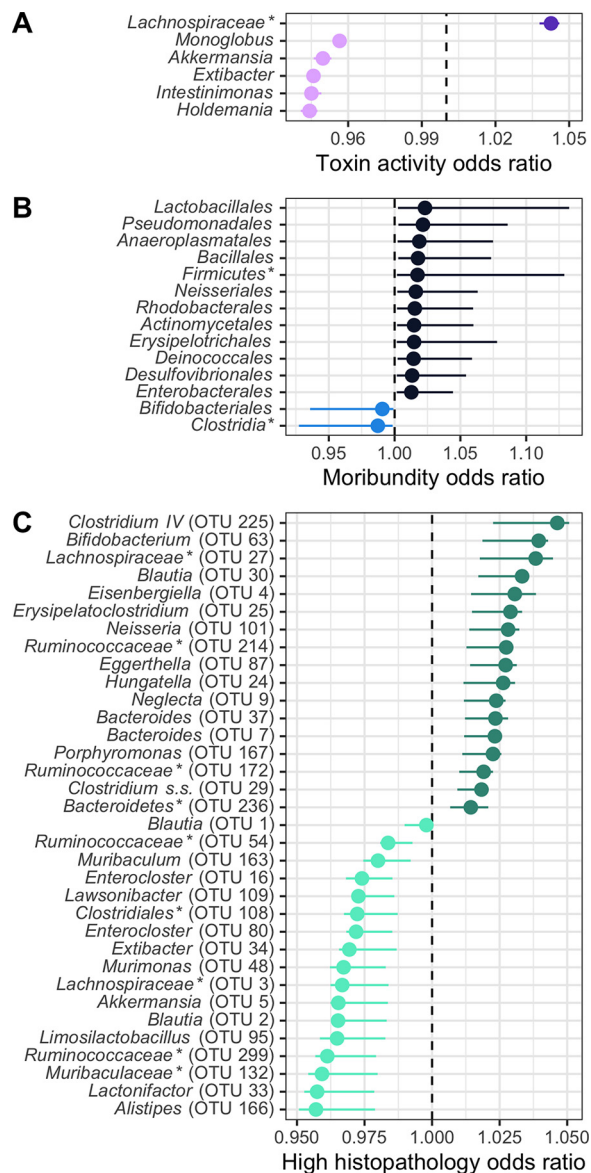
FIG 5 Fecal bacterial community members of the murine gut at the time of *C. difficile* infection predicted outcomes of the infection. On the day of infection (day 0), bacterial community members grouped by different classification rank were modeled with logistic regression to predict the infection outcome. The models used the highest taxonomic classification rank without a decrease in performance. Models used all community members, but plotted are those members with a mean odds ratio not equal to 1. The medians (solid points) and interquartile ranges (lines) of the odds ratio are plotted. Bacterial groups are ordered by their odds ratio. *, bacterial group was unclassified at lower taxonomic classification ranks. (A) Bacterial members grouped by genus predicted which mice would have toxin activity detected at any point throughout the infection. Data with a decreased probability of toxin activity are colored light purple, and those with an increased probability of toxin activity are colored dark purple. (B) Bacterial members grouped by order predicted which mice would become moribund. Data with a decreased probability of moribundity are colored light blue, and those with an increased probability of moribundity are colored dark blue. (C) Bacterial members grouped by OTU predicted if the mice would have a high (greater than the median score of 5) or low (less than the median score of 5) histopathologic summary score. Data with a decreased probability of high histopathologic score are colored light green, and those with an increased probability of high histopathologic score are colored dark green.

The state of the gut bacterial community determines the ability of *C. difficile* to colonize and persist in the intestine. *C. difficile* is unable to colonize an unperturbed healthy murine gut community and is only able to become established after a perturbation (21). Once colonized, the different communities lead to different metabolic responses

(Fig. 4C; see Fig. S4 in the supplemental material). While we did not use IL-10-deficient mice, it is possible the bacterial community and host response are similarly modified by *Helicobacter*, allowing *C. difficile* infection and host damage. Aside from *Helicobacter*, these groups of bacteria that were associated with more severe outcomes did not have a conserved association between their relative abundance and the disease severity across all mice.

Since we observed groups of bacteria that were associated with less-severe disease, it may be appropriate to apply the damage response framework for microbial pathogenesis to CDI (74, 75). This framework posits that disease is not driven by a single entity—rather it is an emergent property of the responses of the host immune system, infecting microbe, *C. difficile*, and the indigenous microbes at the site of infection. In this set of experiments, we used the same host background, C57BL/6 mice, and the same infecting microbe, *C. difficile* RT027 clinical isolate 431, with different gut bacterial communities. The bacterial groups in those communities were often present in both moribund and nonmoribund mice and across the range of histopathologic scores. Thus, it was not merely the presence of the bacteria but their activity in response to the other microbes and host that affected the extent of the host damage. Additionally, while each mouse and *C. difficile* population had the same genetic background, they too were reacting to the specific microbial community. Different gut microbial communities can also have different effects on the host immune responses (76). Disease severity is driven by the cumulative effect of the host immune response and the activity of *C. difficile* and the gut bacteria. *C. difficile* drives host damage through the production of toxin. The gut microbiota can modulate host damage through the balance of metabolic and competitive interactions with *C. difficile*, such as bacteriocin production or mucin degradation, and interactions with the host, such as host mucus glycosylation or intestinal IL-33 expression (15, 77). For example, low levels of mucin degradation can provide nutrients to other community members, producing a diverse nondamaging community (78). However, if mucin degradation becomes too great, it reduces the protective function of the mucin layer and exposes the epithelial cells. This overharvesting can contribute to the host damage due to other members producing toxin. Thus, the resultant intestinal damage is the balance of all activities in the gut environment. Host damage is the emergent property of numerous damage response curves, such as one for host immune response, one for *C. difficile* activity, and another for microbiome community activity, each of which is a composite curve of the individual activities from each group, such as antibody production, neutrophil infiltration, toxin production, sporulation, and fiber and mucin degradation. Therefore, while we have identified populations of interest, it may be necessary to target multiple types of bacteria to reduce the community interactions contributing to host damage.

Here, we have shown several bacterial groups and their relative abundances are associated with variation in CDI disease severity. Further understanding how the microbiome affects severity in patients could reduce the amount of adverse CDI outcomes. When a patient is diagnosed with CDI, the gut community composition, in addition to the traditionally obtained clinical information, may improve our severity prediction and guide prophylactic treatment. Treatment of the microbiome at the time of diagnosis, in addition to *C. difficile*, may prevent the infection from becoming more severe.

MATERIALS AND METHODS

Animal care. Six- to 13-week-old male and female germfree C57BL/6 were obtained from a single breeding colony in the University of Michigan Germ-free Mouse Core. Mice were grouped by bacterial community donor (M1, $n = 3$; M2, $n = 3$; M3, $n = 3$; M4, $n = 3$; M5, $n = 7$; M6, $n = 3$; N1, $n = 11$; N2, $n = 7$; N3, $n = 3$; N4, $n = 3$; N5, $n = 3$; N6, $n = 3$; N7, $n = 7$; N8, $n = 3$; and N9, $n = 2$), housed in cages at 2 to 4 mice per cage, and maintained in germfree isolators at the University of Michigan germfree facility. All mouse experiments were approved by the University Committee on Use and Care of Animals at the University of Michigan.

C. difficile experiments. Human fecal samples were obtained as part of a study by Schubert et al. and selected based on community clusters (18) to result in diverse community structures (see Table S1 in the supplemental material). Feces were homogenized by mixing 200 mg of sample with 5 mL of phosphate-buffered saline (PBS). Mice were inoculated with 100 μL of the fecal homogenate via oral gavage.

Two weeks after the fecal community inoculation, mice were challenged with *C. difficile*. Stool samples from each mouse were collected 1 day prior to *C. difficile* challenge and plated for *C. difficile* enumeration to confirm no *C. difficile* was detected in stool prior to challenge. *C. difficile* clinical isolate 431 came from Carlson et al., had previously been isolated and characterized (35, 36), and was recently further characterized (37). Spore concentrations were determined both before and after challenge (79). A total of 10³ *C. difficile* spores were given to each mouse via oral gavage.

Sample collection. Fecal samples were collected on the day of *C. difficile* challenge and the following 10 days. Each day, a fecal sample was collected and a portion was weighed for plating (approximately 30 mg), and the remaining sample was frozen at $-20°C$. Anaerobically, the weighed fecal samples were serially diluted in PBS, plated on TCCFA plates, and incubated at 37°C for 24 h. The plates were then counted for the number of CFU (80).

DNA sequencing. From the frozen fecal samples, total bacterial DNA was extracted using MoBio PowerSoil-htp 96-well soil DNA isolation kit. We amplified the 16S rRNA gene V4 region and sequenced the resulting amplicons using an Illumina MiSeq sequencer, as described previously (81).

Sequence curation. Sequences were processed with mothur (v.1.44.3), as previously described (81, 82). In short, we used a 3% dissimilarity cutoff to group sequences into operational taxonomic units (OTUs). We used a naive Bayesian classifier with the Ribosomal Database Project training set (version 18) to assign taxonomic classifications to each OTU (83). We sequenced a mock community of a known community composition and 16S rRNA gene sequences. We processed this mock community with our samples to calculate the error rate for our sequence curation, which was 0.19%.

Toxin cytotoxicity assay. To prepare a sample for the activity assay, fecal material was diluted 1:10 (wt/vol) using sterile PBS and then filter sterilized through a 0.22-μm-pore filter. Toxin activity was assessed using a Vero cell rounding-based cytotoxicity assay, as described previously (30). The cytotoxicity titer for each sample was determined as the last dilution that resulted in at least 80% cell rounding. Toxin titers are reported as the $\log_{10}$ value of the reciprocal of the cytotoxicity titer.

Histopathology evaluation. Mouse cecal tissue was placed in histopathology cassettes and fixed in 10% formalin, and then the samples were stored in 70% ethanol. McClinchey Histology Labs, Inc. (Stockbridge, MI), embedded the samples in paraffin, sectioned them, and created the hematoxylin- and eosin-stained slides. The slides were scored using previously described criteria by a board-certified veterinary pathologist who was blind to the experimental groups (30). Slides were scored as 0 to 4 for parameters of epithelial damage, tissue edema, and inflammation, and a summary score of 0 to 12 was generated by summing the three individual parameter scores. For nonmoribund mice, histopathological summary scores used for LEfSe and logistic regression were split into high and low groups based on greater or less than the median summary score of 5 because they had a bimodal distribution ($P < 0.05$).

Statistical analysis and modeling. To compare community structures, we calculated Yue and Clayton dissimilarity matrices (θ_{YC}) in mothur (84). For this calculation, we averaged 1,000 subsamples or rarified samples to 2,107 sequence reads per sample to limit uneven sampling biases. We tested for differences in individual taxonomic groups that would explain the outcome differences with LEfSe (85) in mothur (using default parameters with an LDA of >4). We tested for differences in temporal trends through fitting a linear regression model to each OTU and tested for differences in regression coefficients by histopathological summary scores with LEfSe (85) in mothur (using default parameters with an LDA of >3). The remaining statistical analysis and data visualization were performed in R (v4.0.5) with the tidyverse package (v1.3.1). We tested for significant differences in β diversity (θ_{YC}), histopathological scores, and toxin activity using the Wilcoxon rank sum test, nonunimodality to the nonmoribund histopathological summary score using Hartigans' dip test, and toxin detection in mice using the Pearson's chi-square test. We used Spearman's correlation to identify which OTUs that had a correlation between their relative abundance and the histopathologic summary score. P values were then corrected for multiple comparisons with a Benjamini and Hochberg adjustment for a type I error rate of 0.05 (86). We built L2 logistic regression models using the mikropml package (87). Sequence counts were summed by taxonomic ranks from day 0 samples and normalized by centering to the feature mean and scaling by the standard deviation, and features positively or negatively correlated were collapsed into a single feature. For each L2 logistic regression model, we ran 100 random iterations using values of 1e0, 1e1, 1e2, 2e2, 3e2, 4e2, 5e2, 6e2, 7e2, 8e2, 9e2, 1e3, and 1e4 for the L2 regularization penalty, with a split of 80% of the data for training and 20% of the data for testing. Finally, we did not compare murine communities to donor community or clinical data because germfree mice colonized with nonmurine fecal communities have been shown to more closely resemble the murine communities than the donor species community (88). Furthermore, it is not our intention to make any inferences regarding human-associated bacteria and their relationship with human CDI outcome.

Code availability. Scripts necessary to reproduce our analysis and this article are available in the GitHub online repository (https://github.com/SchlossLab/Lesniak_Severity_mBio_2022).

Accession number(s). All 16S rRNA gene sequence data and associated metadata are available through the Sequence Read Archive via accession no. PRJNA787941.

SUPPLEMENTAL MATERIAL

Supplemental material is available online only.

FIG S1, TIF file, 0.1 MB.

FIG S2, TIF file, 0.3 MB.

FIG S3, TIF file, 0.6 MB.

FIG S4, TIF file, 2 MB.
TABLE S1, PDF file, 0.02 MB.

REFERENCES

1. Kelly CP, LaMont JT. 2008. *Clostridium difficile*—more difficult than ever. N Engl J Med 359:1932–1940. https://doi.org/10.1056/NEJMra0707500.
2. McDonald LC, Gerding DN, Johnson S, Bakken JS, Carroll KC, Coffin SE, Dubberke ER, Garey KW, Gould CV, Kelly C, Loo V, Sammons JS, Sandora TJ, Wilcox MH. 2018. Clinical practice guidelines for *Clostridium difficile* infection in adults and children: 2017 update by the Infectious Diseases Society of America (IDSA) and Society for Healthcare Epidemiology of America (SHEA). Clin Infect Dis 66:e1–e48. https://doi.org/10.1093/cid/cix1085.
3. Perry DA, Shirley D, Micic D, Patel CP, Putler R, Menon A, Young VB, Rao K. 2021. External validation and comparison of *Clostridioides difficile* severity scoring systems. Clin Infect Dis 74:2028–2035. https://doi.org/10.1093/cid/ciab737.
4. Buffie CG, Bucci V, Stein RR, McKenney PT, Ling L, Gobourne A, No D, Liu H, Kinnebrew M, Viale A, Littmann E, van den Brink MRM, Jenq RR, Taur Y, Sander C, Cross JR, Toussaint NC, Xavier JB, Pamer EG. 2015. Precision microbiome reconstitution restores bile acid mediated resistance to *Clostridium difficile*. Nature 517:205–208. https://doi.org/10.1038/nature13828.
5. Britton RA, Young VB. 2014. Role of the intestinal microbiota in resistance to colonization by *Clostridium difficile*. Gastroenterology 146:1547–1553. https://doi.org/10.1053/j.gastro.2014.01.059.
6. Hryckowian AJ, Treuren WV, Smits SA, Davis NM, Gardner JO, Bouley DM, Sonnenburg JL. 2018. Microbiota-accessible carbohydrates suppress *Clostridium difficile* infection in a murine model. Nat Microbiol 3:662–669. https://doi.org/10.1038/s41564-018-0150-6.
7. Vila AV, Collij V, Sanna S, Sinha T, Imhann F, Bourgonje AR, Mujagic Z, Jonkers DMAE, Masclee AAM, Fu J, Kurilshikov A, Wijmenga C, Zhernakova A, Weersma RK. 2020. Impact of commonly used drugs on the composition and metabolic function of the gut microbiota. Nat Commun 11:362. https://doi.org/10.1038/s41467-019-14177-z.
8. Abbas A, Zackular JP. 2020. Microbe-microbe interactions during *Clostridioides difficile* infection. Curr Opin Microbiol 53:19–25. https://doi.org/10.1016/j.mib.2020.01.016.
9. Jenior ML, Leslie JL, Young VB, Schloss PD. 2017. *Clostridium difficile* colonizes alternative nutrient niches during infection across distinct murine gut microbiomes. mSystems 2:e00063-17. https://doi.org/10.1128/mSystems.00063-17.
10. Sorg JA, Sonenshein AL. 2008. Bile salts and glycine as cogerminants for *Clostridium difficile* spores. J Bacteriol 190:2505–2512. https://doi.org/10.1128/JB.01765-07.
11. Thanissery R, Winston JA, Theriot CM. 2017. Inhibition of spore germination, growth, and toxin activity of clinically relevant *C. difficile* strains by gut microbiota derived secondary bile acids. Anaerobe 45:86–100. https://doi.org/10.1016/j.anaerobe.2017.03.004.

12. Aguirre AM, Yalcinkaya N, Wu Q, Swennes A, Tessier ME, Roberts P, Miyajima F, Savidge T, Sorg JA. 2021. Bile acid-independent protection against *Clostridioides difficile* infection. PLoS Pathog 17:e1010015. https://doi.org/10.1371/journal.ppat.1010015.
13. Kang JD, Myers CJ, Harris SC, Kakiyama G, Lee I-K, Yun B-S, Matsuzaki K, Furukawa M, Min H-K, Bajaj JS, Zhou H, Hylemon PB. 2019. Bile acid 7α-dehydroxylating gut bacteria secrete antibiotics that inhibit *Clostridium difficile*: role of secondary bile acids. Cell Chem Biol 26:27–34.e4. https://doi.org/10.1016/j.chembiol.2018.10.003.
14. Leslie JL, Jenior ML, Vendrov KC, Standke AK, Barron MR, O'Brien TJ, Unverdorben L, Thaprawat P, Bergin IL, Schloss PD, Young VB. 2021. Protection from lethal *Clostridioides difficile* infection via intraspecies competition for cogerminant. mBio 12:e00522-21. https://doi.org/10.1128/mBio.00522-21.
15. Nagao-Kitamoto H, Leslie JL, Kitamoto S, Jin C, Thomsson KA, Gillilland MG, Kuffa P, Goto Y, Jenq RR, Ishii C, Hirayama A, Seekatz AM, Martens EC, Eaton KA, Kao JY, Fukuda S, Higgins PDR, Karlsson NG, Young VB, Kamada N. 2020. Interleukin-22-mediated host glycosylation prevents *Clostridioides difficile* infection by modulating the metabolic activity of the gut microbiota. Nat Med 26:608–617. https://doi.org/10.1038/s41591-020-0764-0.
16. Tomkovich S, Stough JMA, Bishop L, Schloss PD. 2020. The initial gut microbiota and response to antibiotic perturbation influence *Clostridioides difficile* clearance in mice. mSphere 5:e00869-20. https://doi.org/10.1128/mSphere.00869-20.
17. Nagpal R, Wang S, Woods LCS, Seshie O, Chung ST, Shively CA, Register TC, Craft S, McClain DA, Yadav H. 2018. Comparative microbiome signatures and short-chain fatty acids in mouse, rat, non-human primate, and human feces. Front Microbiol 9:2897. https://doi.org/10.3389/fmicb.2018.02897.
18. Schubert AM, Rogers MAM, Ring C, Mogle J, Petrosino JP, Young VB, Aronoff DM, Schloss PD. 2014. Microbiome data distinguish patients with *Clostridium difficile* infection and non-*C. difficile*-associated diarrhea from healthy controls. mBio 5:e01021-14. https://doi.org/10.1128/mBio.01021-14.
19. Gillilland MG, Erb-Downward JR, Bassis CM, Shen MC, Toews GB, Young VB, Huffnagle GB. 2012. Ecological succession of bacterial communities during conventionalization of germ-free mice. Appl Environ Microbiol 78:2359–2366. https://doi.org/10.1128/AEM.05239-11.
20. Chen X, Katchar K, Goldsmith JD, Nanthakumar N, Cheknis A, Gerding DN, Kelly CP. 2008. A mouse model of *Clostridium difficile*-associated disease. Gastroenterology 135:1984–1992. https://doi.org/10.1053/j.gastro.2008.09.002.
21. Schubert AM, Sinani H, Schloss PD. 2015. Antibiotic-induced alterations of the murine gut microbiota and subsequent effects on colonization resistance against *Clostridium difficile*. mBio 6:e00974-15. https://doi.org/10.1128/mBio.00974-15.

22. Cowardin CA, Buonomo EL, Saleh MM, Wilson MG, Burgess SL, Kuehne SA, Schwan C, Eichhoff AM, Koch-Nolte F, Lyras D, Aktories K, Minton NP, Petri WA. 2016. The binary toxin CDT enhances *Clostridium difficile* virulence by suppressing protective colonic eosinophilia. Nat Microbiol 1:16108. https://doi.org/10.1038/nmicrobiol.2016.108.

23. Seekatz AM, Rao K, Santhosh K, Young VB. 2016. Dynamics of the fecal microbiome in patients with recurrent and nonrecurrent *Clostridium difficile* infection. Genome Med 8:47. https://doi.org/10.1186/s13073-016-0298-8.

24. Dieterle MG, Putler R, Perry DA, Menon A, Abernathy-Close L, Perlman NS, Penkevich A, Standke A, Keidan M, Vendrov KC, Bergin IL, Young VB, Rao K. 2020. Systemic inflammatory mediators are effective biomarkers for predicting adverse outcomes in *Clostridioides difficile* infection. mBio 11:e00180-20. https://doi.org/10.1128/mBio.00180-20.

25. Lesniak NA, Leboffe L, Schubert AM, Sinani H, Schloss PD. 2021. Clearance of *Clostridioides difficile* colonization is associated with antibiotic-specific bacterial changes. mSphere 6:e01238-20. https://doi.org/10.1128/mSphere.01238-20.

26. Lungulescu OA, Cao W, Gatskevich E, Tlhabano L, Stratidis JG. 2011. CSI: a severity index for *Clostridium difficile* infection at the time of admission. J Hosp Infect 79:151–154. https://doi.org/10.1016/j.jhin.2011.04.017.

27. Zar FA, Bakkanagari SR, Moorthi K, Davis MB. 2007. A comparison of vancomycin and metronidazole for the treatment of *Clostridium difficile*-associated diarrhea, stratified by disease severity. Clin Infect Dis 45:302–307. https://doi.org/10.1086/519265.

28. di Masi A, Leboffe L, Polticelli F, Tonon F, Zennaro C, Caterino M, Stano P, Fischer S, Hägele M, Müller M, Kleger A, Papatheodorou P, Nocca G, Arcovito A, Gori A, Ruoppolo M, Barth H, Petrosillo N, Ascenzi P, Bella SD. 2018. Human serum albumin is an essential component of the host defense mechanism against *Clostridium difficile* intoxication. J Infect Dis 218:1424–1435. https://doi.org/10.1093/infdis/jiy338.

29. Abernathy-Close L, Dieterle MG, Vendrov KC, Bergin IL, Rao K, Young VB. 2020. Aging dampens the intestinal innate immune response during severe *Clostridioides difficile* infection and is associated with altered cytokine levels and granulocyte mobilization. Infect Immun 88:e00960-19. https://doi.org/10.1128/IAI.00960-19.

30. Theriot CM, Koumpouras CC, Carlson PE, Bergin II, Aronoff DM, Young VB. 2011. Cefoperazone-treated mice as an experimental platform to assess differential virulence of *Clostridium difficile* strains. Gut Microbes 2:326–334. https://doi.org/10.4161/gmic.19142.

31. Goorhuis A, Bakker D, Corver J, Debast SB, Harmanus C, Notermans DW, Bergwerff AA, Dekker FW, Kuijper EJ. 2008. Emergence of *Clostridium difficile* infection due to a new hypervirulent strain, polymerase chain reaction ribotype 078. Clin Infect Dis 47:1162–1170. https://doi.org/10.1086/592257.

32. O'Connor JR, Johnson S, Gerding DN. 2009. *Clostridium difficile* infection caused by the epidemic BI/NAP1/027 strain. Gastroenterology 136:1913–1924. https://doi.org/10.1053/j.gastro.2009.02.073.

33. Rao K, Micic D, Natarajan M, Winters S, Kiel MJ, Walk ST, Santhosh K, Mogle JA, Galecki AT, LeBar W, Higgins PDR, Young VB, Aronoff DM. 2015. *Clostridium difficile* ribotype 027: relationship to age, detectability of toxins A or B in stool with rapid testing, severe infection, and mortality. Clin Infect Dis 61:233–241. https://doi.org/10.1093/cid/civ254.

34. Walk ST, Micic D, Jain R, Lo ES, Trivedi I, Liu EW, Almassalha LM, Ewing SA, Ring C, Galecki AT, Rogers MAM, Washer L, Newton DW, Malani PN, Young VB, Aronoff DM. 2020. *Clostridium difficile* ribotype does not predict severe infection. Gut Microbes 12:1661–1668. https://doi.org/10.1093/cid/cis786.

35. Carlson PE, Walk ST, Bourgis AET, Liu MW, Kopliku F, Lo E, Young VB, Aronoff DM, Hanna PC. 2013. The relationship between phenotype, ribotype, and clinical disease in human *Clostridium difficile* isolates. Anaerobe 24:109–116. https://doi.org/10.1016/j.anaerobe.2013.04.003.

36. Carlson PE, Kaiser AM, McColm SA, Bauer JM, Young VB, Aronoff DM, Hanna PC. 2015. Variation in germination of *Clostridium difficile* clinical isolates correlates to disease severity. Anaerobe 33:64–70. https://doi.org/10.1016/j.anaerobe.2015.02.003.

37. Saund K, Pirani A, Lacy B, Hanna PC, Snitkin ES. 2021. Strain variation in Clostridioides difficile toxin activity associated with genomic variation at both PaLoc and non-PaLoc loci. bioRxiv. https://doi.org/10.1101/2021.12.08.471880.

38. He M, Sebaihia M, Lawley TD, Stabler RA, Dawson LF, Martin MJ, Holt KE, Seth-Smith HMB, Quail MA, Rance R, Brooks K, Churcher C, Harris D, Bentley SD, Burrows C, Clark L, Corton C, Murray V, Rose G, Thurston S, van Tonder A, Walker D, Wren BW, Dougan G, Parkhill J. 2010. Evolutionary dynamics of *Clostridium difficile* over short and long time scales. Proc Natl Acad Sci U S A 107:7527–7532. https://doi.org/10.1073/pnas.0914322107.

39. Butt E, Foster JA, Keedwell E, Bell JE, Titball RW, Bhangu A, Michell SL, Sheridan R. 2013. Derivation and validation of a simple, accurate and robust prediction rule for risk of mortality in patients with *Clostridium difficile* infection. BMC Infect Dis 13:316. https://doi.org/10.1186/1471-2334-13-316.

40. van Beurden YH, Hensgens MPM, Dekkers OM, Cessie SL, Mulder CJJ, Vandenbroucke-Grauls CMJE. 2017. External validation of three prediction tools for patients at risk of a complicated course of *Clostridium difficile* infection: disappointing in an outbreak setting. Infect Control Hosp Epidemiol 38:897–905. https://doi.org/10.1017/ice.2017.89.

41. Jenior ML, Leslie JL, Young VB, Schloss PD. 2018. *Clostridium difficile* alters the structure and metabolism of distinct cecal microbiomes during initial infection to promote sustained colonization. mSphere 3:e00261-18. https://doi.org/10.1128/mSphere.00261-18.

42. Staley C, Weingarden AR, Khoruts A, Sadowsky MJ. 2017. Interaction of gut microbiota with bile acid metabolism and its influence on disease states. Appl Microbiol Biotechnol 101:47–64. https://doi.org/10.1007/s00253-016-8006-6.

43. Long SL, Gahan CGM, Joyce SA. 2017. Interactions between gut bacteria and bile in health and disease. Mol Aspects Med 56:54–65. https://doi.org/10.1016/j.mam.2017.06.002.

44. Sorg JA, Sonenshein AL. 2010. Inhibiting the initiation of *Clostridium difficile* spore germination using analogs of chenodeoxycholic acid, a bile acid. J Bacteriol 192:4983–4990. https://doi.org/10.1128/JB.00610-10.

45. Dubois T, Tremblay YDN, Hamiot A, Martin-Verstraete I, Deschamps J, Monot M, Briandet R, Dupuy B. 2019. A microbiota-generated bile salt induces biofilm formation in *Clostridium difficile*. NPJ Biofilms Microbiomes 5:14. https://doi.org/10.1038/s41522-019-0087-4.

46. Ng KM, Ferreyra JA, Higginbottom SK, Lynch JB, Kashyap PC, Gopinath S, Naidu N, Choudhury B, Weimer BC, Monack DM, Sonnenburg JL. 2013. Microbiota-liberated host sugars facilitate post-antibiotic expansion of enteric pathogens. Nature 502:96–99. https://doi.org/10.1038/nature12503.

47. Ferreyra JA, Wu KJ, Hryckowian AJ, Bouley DM, Weimer BC, Sonnenburg JL. 2014. Gut microbiota-produced succinate promotes *C. difficile* infection after antibiotic treatment or motility disturbance. Cell Host Microbe 16:770–777. https://doi.org/10.1016/j.chom.2014.11.003.

48. Martin-Verstraete I, Peltier J, Dupuy B. 2016. The regulatory networks that control *Clostridium difficile* toxin synthesis. Toxins 8:153. https://doi.org/10.3390/toxins8050153.

49. Lawley TD, Clare S, Walker AW, Stares MD, Connor TR, Raisen C, Goulding D, Rad R, Schreiber F, Brandt C, Deakin LJ, Pickard DJ, Duncan SH, Flint HJ, Clark TG, Parkhill J, Dougan G. 2012. Targeted restoration of the intestinal microbiota with a simple, defined bacteriotherapy resolves relapsing *Clostridium difficile* disease in mice. PLoS Pathog 8:e1002995. https://doi.org/10.1371/journal.ppat.1002995.

50. Reeves AE, Theriot CM, Bergin IL, Huffnagle GB, Schloss PD, Young VB. 2011. The interplay between microbiome dynamics and pathogen dynamics in a murine model of *Clostridium difficile* infection. Gut Microbes 2:145–158. https://doi.org/10.4161/gmic.2.3.16333.

51. Battaglioli EJ, Hale VL, Chen J, Jeraldo P, Ruiz-Mojica C, Schmidt BA, Rekdal VM, Till LM, Huq L, Smits SA, Moor WJ, Jones-Hall Y, Smyrk T, Khanna S, Pardi DS, Grover M, Patel R, Chia N, Nelson H, Sonnenburg JL, Farrugia G, Kashyap PC. 2018. *Clostridioides difficile* uses amino acids associated with gut microbial dysbiosis in a subset of patients with diarrhea. Sci Transl Med 10:eaam7019. https://doi.org/10.1126/scitranslmed.aam7019.

52. Liu X, Mao B, Gu J, Wu J, Cui S, Wang G, Zhao J, Zhang H, Chen W. 2021. *Blautia*—a new functional genus with potential probiotic properties? Gut Microbes 13:1–21. https://doi.org/10.1080/19490976.2021.1875796.

53. Mabrok HB, Klopfleisch R, Ghanem KZ, Clavel T, Blaut M, Loh G. 2012. Lignan transformation by gut bacteria lowers tumor burden in a gnotobiotic rat model of breast cancer. Carcinogenesis 33:203–208. https://doi.org/10.1093/carcin/bgr256.

54. Kim CC, Healey GR, Kelly WJ, Patchett ML, Jordens Z, Tannock GW, Sims IM, Bell TJ, Hedderley D, Henrissat B, Rosendale DI. 2019. Genomic insights from *Monoglobus pectinilyticus*: a pectin-degrading specialist bacterium in the human colon. ISME J 13:1437–1456. https://doi.org/10.1038/s41396-019-0363-6.

55. Choi S-H, Kim J-S, Park J-E, Lee KC, Eom MK, Oh BS, Yu SY, Kang SW, Han K-I, Suh MK, Lee DH, Yoon H, Kim B-Y, Lee JH, Lee JH, Lee J-S, Park S-H. 2019. *Anaerotignum faecicola* sp. nov., isolated from human faeces. J Microbiol 57:1073–1078. https://doi.org/10.1007/s12275-019-9268-3.

56. Ueki A, Goto K, Ohtaki Y, Kaku N, Ueki K. 2017. Description of *Anaerotignum aminivorans* gen. nov., sp. nov., a strictly anaerobic, amino-acid-decomposing bacterium isolated from a methanogenic reactor, and reclassification of

Clostridium propionicum, *Clostridium neopropionicum* and *Clostridium lactatifermentans* as species of the genus *Anaerotignum*. Int J Syst Evol Microbiol 67:4146–4153. https://doi.org/10.1099/ijsem.0.002268.

57. Stein RR, Bucci V, Toussaint NC, Buffie CG, Rätsch G, Pamer EG, Sander C, Xavier JB. 2013. Ecological modeling from time-series inference: insight into dynamics and stability of intestinal microbiota. PLoS Comput Biol 9: e1003388. https://doi.org/10.1371/journal.pcbi.1003388.

58. Nakashima T, Fujii K, Seki T, Aoyama M, Azuma A, Kawasome H. 2021. Novel gut microbiota modulator, which markedly increases *Akkermansia muciniphila* occupancy, ameliorates experimental colitis in rats. Dig Dis Sci https://doi.org/10.1007/s10620-021-07131-x.

59. Geerlings S, Kostopoulos I, de Vos WM, Belzer C. 2018. *Akkermansia muciniphila* in the human gastrointestinal tract: when, where, and how? Microorganisms 6:75. https://doi.org/10.3390/microorganisms6030075.

60. Deng H, Yang S, Zhang Y, Qian K, Zhang Z, Liu Y, Wang Y, Bai Y, Fan H, Zhao X, Zhi F. 2019. *Bacteroides fragilis* prevents *Clostridium difficile* infection in a mouse model by restoring gut barrier and microbiome regulation. Front Microbiol 10:601. https://doi.org/10.3389/fmicb.2019.00601.

61. Engevik MA, Engevik AC, Engevik KA, Auchtung JM, Chang-Graham AL, Ruan W, Luna RA, Hyser JM, Spinler JK, Versalovic J. 2021. Mucin-degrading microbes release monosaccharides that chemoattract *Clostridioides difficile* and facilitate colonization of the human intestinal mucus layer. ACS Infect Dis 7:1126–1142. https://doi.org/10.1021/acsinfecdis.0c00634.

62. Reeves AE, Koenigsknecht MJ, Bergin IL, Young VB. 2012. Suppression of *Clostridium difficile* in the gastrointestinal tracts of germfree mice inoculated with a murine isolate from the family *Lachnospiraceae*. Infect Immun 80:3786–3794. https://doi.org/10.1128/IAI.00647-12.

63. Ma L, Keng J, Cheng M, Pan H, Feng B, Hu Y, Feng T, Yang F. 2021. Gut microbiome and serum metabolome alterations associated with isolated dystonia. mSphere 6:e00283-21. https://doi.org/10.1128/mSphere.00283-21.

64. Haas KN, Blanchard JL. 2020. Reclassification of the *Clostridium clostridioforme* and *Clostridium sphenoides* clades as *Enterocloster* gen. nov. and *Lacrimispora* gen. nov., including reclassification of 15 taxa. Int J Syst Evol Microbiol 70:23–34. https://doi.org/10.1099/ijsem.0.003698.

65. Finegold SM, Song Y, Liu C, Hecht DW, Summanen P, Könönen E, Allen SD. 2005. *Clostridium clostridioforme*: a mixture of three clinically important species. Eur J Clin Microbiol Infect Dis 24:319–324. https://doi.org/10.1007/s10096-005-1334-6.

66. Tomkovich S, Taylor A, King J, Colovas J, Bishop L, McBride K, Royzenblat S, Lesniak NA, Bergin IL, Schloss PD. 2021. An osmotic laxative renders mice susceptible to prolonged *Clostridioides difficile* colonization and hinders clearance. mSphere 6:e00629-21. https://doi.org/10.1128/mSphere.00629-21.

67. Keith JW, Dong Q, Sorbara MT, Becattini S, Sia JK, Gjonbalaj M, Seok R, Leiner IM, Littmann ER, Pamer EG. 2020. Impact of antibiotic-resistant bacteria on immune activation and *Clostridioides difficile* infection in the mouse intestine. Infect Immun 88:e00362-19. https://doi.org/10.1128/IAI.00362-19.

68. Zackular JP, Moore JL, Jordan AT, Juttukonda LJ, Noto MJ, Nicholson MR, Crews JD, Semler MW, Zhang Y, Ware LB, Washington MK, Chazin WJ, Caprioli RM, Skaar EP. 2016. Dietary zinc alters the microbiota and decreases resistance to *Clostridium difficile* infection. Nat Med 22: 1330–1334. https://doi.org/10.1038/nm.4174.

69. Berkell M, Mysara M, Xavier BB, van Werkhoven CH, Monsieurs P, Lammens C, Ducher A, Vehreschild MJGT, Goossens H, de Gunzburg J, Bonten MJM, Malhotra-Kumar S. 2021. Microbiota-based markers predictive of development of *Clostridioides difficile* infection. Nat Commun 12: 2241. https://doi.org/10.1038/s41467-021-22302-0.

70. Gardiner BJ, Tai AY, Kotsanas D, Francis MJ, Roberts SA, Ballard SA, Junckerstorff RK, Korman TM. 2015. Clinical and microbiological characteristics of *Eggerthella lenta* bacteremia. J Clin Microbiol 53:626–635. https://doi.org/10.1128/JCM.02926-14.

71. Iljazovic A, Roy U, Gálvez EJC, Lesker TR, Zhao B, Gronow A, Amend L, Will SE, Hofmann JD, Pils MC, Schmidt-Hohagen K, Neumann-Schaal M, Strowig T. 2021. Perturbation of the gut microbiome by *Prevotella* spp. enhances host susceptibility to mucosal inflammation. Mucosal Immunol 14:113–124. https://doi.org/10.1038/s41385-020-0296-4.

72. Nagalingam NA, Robinson CJ, Bergin IL, Eaton KA, Huffnagle GB, Young VB. 2013. The effects of intestinal microbial community structure on disease manifestation in IL-10$^{-/-}$ mice infected with *Helicobacter hepaticus*. Microbiome 1:15. https://doi.org/10.1186/2049-2618-1-15.

73. Abernathy-Close L, Barron MR, George JM, Dieterle MG, Vendrov KC, Bergin IL, Young VB. 2021. Intestinal inflammation and altered gut microbiota associated with inflammatory bowel disease render mice susceptible to *Clostridioides difficile* colonization and infection. mBio 12:e02733-20. https://doi.org/10.1128/mBio.02733-20.

74. Pirofski L-a, Casadevall A. 2008. The damage-response framework of microbial pathogenesis and infectious diseases. Adv Exp Med Biol 635: 135–146. https://doi.org/10.1007/978-0-387-09550-9_11.

75. Casadevall A, Pirofski L-a. 2015. What is a host? Incorporating the microbiota into the damage-response framework. Infect Immun 83:2–7. https://doi.org/10.1128/IAI.02627-14.

76. Lundberg R, Toft MF, Metzdorff SB, Hansen CHF, Licht TR, Bahl MI, Hansen AK. 2020. Human microbiota-transplanted C57BL/6 mice and offspring display reduced establishment of key bacteria and reduced immune stimulation compared to mouse microbiota-transplantation. Sci Rep 10:7805. https://doi.org/10.1038/s41598-020-64703-z.

77. Frisbee AL, Saleh MM, Young MK, Leslie JL, Simpson ME, Abhyankar MM, Cowardin CA, Ma JZ, Pramoonjago P, Turner SD, Liou AP, Buonomo EL, Petri WA. 2019. IL-33 drives group 2 innate lymphoid cell-mediated protection during *Clostridium difficile* infection. Nat Commun 10:2712. https://doi.org/10.1038/s41467-019-10733-9.

78. Tailford LE, Crost EH, Kavanaugh D, Juge N. 2015. Mucin glycan foraging in the human gut microbiome. Front Genet 6:81. https://doi.org/10.3389/fgene.2015.00081.

79. Sorg JA, Dineen SS. 2009. Laboratory maintenance of *Clostridium difficile*. Curr Protoc Microbiol Chapter 9:Unit9A.1. https://doi.org/10.1002/9780471729259.mc09a01s12.

80. Winston JA, Thanissery R, Montgomery SA, Theriot CM. 2016. Cefoperazone-treated mouse model of clinically-relevant *Clostridium difficile* strain R20291. J Vis Exp. https://doi.org/10.3791/54850.

81. Kozich JJ, Westcott SL, Baxter NT, Highlander SK, Schloss PD. 2013. Development of a dual-index sequencing strategy and curation pipeline for analyzing amplicon sequence data on the MiSeq Illumina sequencing platform. Appl Environ Microbiol 79:5112–5120. https://doi.org/10.1128/AEM.01043-13.

82. Schloss PD, Westcott SL, Ryabin T, Hall JR, Hartmann M, Hollister EB, Lesniewski RA, Oakley BB, Parks DH, Robinson CJ, Sahl JW, Stres B, Thallinger GG, Horn DJV, Weber CF. 2009. Introducing mothur: open-source, platform-independent, community-supported software for describing and comparing microbial communities. Appl Environ Microbiol 75:7537–7541. https://doi.org/10.1128/AEM.01541-09.

83. Wang Q, Garrity GM, Tiedje JM, Cole JR. 2007. Naïve Bayesian classifier for rapid assignment of rRNA sequences into the new bacterial taxonomy. Appl Environ Microbiol 73:5261–5267. https://doi.org/10.1128/AEM.00062-07.

84. Yue JC, Clayton MK. 2005. A similarity measure based on species proportions. Commun Stat Theory Methods 34:2123–2131. https://doi.org/10.1080/STA-200066418.

85. Segata N, Izard J, Waldron L, Gevers D, Miropolsky L, Garrett WS, Huttenhower C. 2011. Metagenomic biomarker discovery and explanation. Genome Biol 12:R60. https://doi.org/10.1186/gb-2011-12-6-r60.

86. Benjamini Y, Hochberg Y. 1995. Controlling the false discovery rate: a practical and powerful approach to multiple testing. J R Stat Soc Series B Methodol 57:289–300. https://doi.org/10.1111/j.2517-6161.1995.tb02031.x.

87. Topçuoğlu B, Lapp Z, Sovacool K, Snitkin E, Wiens J, Schloss P. 2021. Mikropml: user-friendly R package for supervised machine learning pipelines. J Open Source Softw 6:3073. https://doi.org/10.21105/joss.03073.

88. Rawls JF, Mahowald MA, Ley RE, Gordon JI. 2006. Reciprocal gut microbiota transplants from zebrafish and mice to germ-free recipients reveal host habitat selection. Cell 127:423–433. https://doi.org/10.1016/j.cell.2006.08.043.